Uncertainty Quantification for Ice Accretion and Cargo Hold Fires

Anthony DeGennaro
Mark Lohry
Clarence W. Rowley III
Luigi Martinelli
Princeton University

FAA JUP Winter 2016 Quarterly Meeting
Atlantic City, NJ
January 2016

Outline

1. Icing: Introduction/Methodology
2. Icing: UQ Examples
3. Icing: Computational-Based UQ
4. Fires: Introduction/Methodology
5. Fires: Example study

Topic

1. Icing: Introduction/Methodology
2. Icing: UQ Examples
3. Icing: Computational-Based UQ
4. Fires: Introduction/Methodology
5. Fires: Example study

Introduction

Motivation

- Wing icing is a serious issue for pilots
  - Massive flow separation, lower lift + higher drag
  - Unpredictable stall
- Wing ice shapes exhibit wide variation, sensitivity to physical parameters
  - Complex physics (coupled airflow-thermodynamics)
  - Uncertainty in physical parameters

Research Goals

- How can observed variations in ice shape be modeled efficiently with a low number of parameters?
- How does uncertainty in the ice shape create uncertainty in aerodynamic performance?

Experimental/Computational Variation in Ice Shape

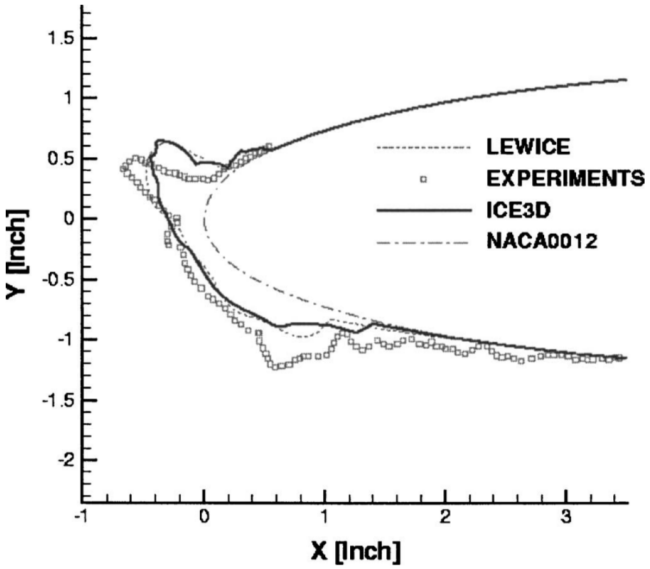

(a) Habashi, 2006

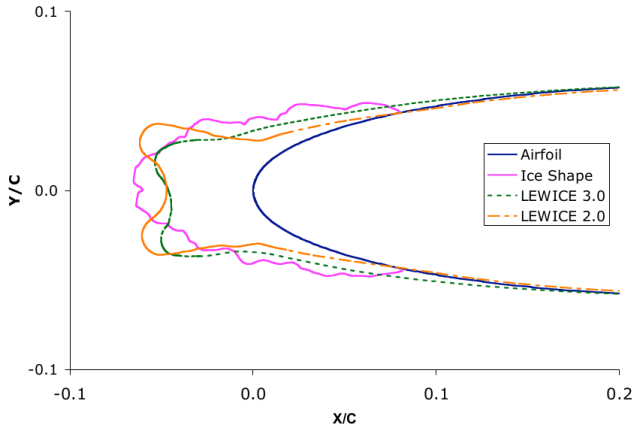

(b) Wright, 2004

- Wide variation in experimental/computational ice shapes[1, 2]
- Suggests sensitivity to perturbations in underlying physical processes
- *UQ approach:* parameterize the shape variation and study its effects on aerodynamics

[1] Beaugendre H., Morency M., and Habashi W.G. *Development of a Second Generation in-Flight Icing Simulation Code*. Journal of Fluids Engineering, ASME, 2006.

[2] Wright W. and Potapczuk, M.G. *Semi-Empirical Modeling of SLD Physics*, AIAA 2004-412. 42nd AIAA Aerospace Sciences Meeting, Reno, NV, 2004.

Input-Process Modeling

- **Heuristic**
  - Ice shape parameters are selected by intuition
  - Examples: horn height, angle
- **Data-Based: Proper Orthogonal Decomposition** [3]
  - Analyze database of M shapes from experiments/simulations
  - Each individual ice shape can be represented by a vector $\mathbf{x} \in \mathbb{R}^N$
  - Approximate $\mathbf{x}$ using some basis vectors ψ_i:

$$\mathbf{x} \approx \sum_{i=1}^{P} a_i \psi_i$$

  - Choose basis vectors to be the eigenvectors of the dataset covariance matrix

$$\mathcal{R}\psi_k = \lambda_k \psi_k \text{ where:}$$

$$\mathcal{R} = \frac{1}{M}\mathbf{X}\mathbf{X}^T \text{ and: } \mathbf{X} = \begin{bmatrix} | & & | \\ x_1 & \cdots & x_M \\ | & & | \end{bmatrix}$$

[3] Holmes P. et. al. *Turbulence, Coherent Structures, Dynamical Systems and Symmetry*, Cambridge University Press, New York, 2012.

Polynomial Chaos Expansions (PCE)

- **Polynomial Chaos Framework** [4]
  - Let $\mathbf{Z} = (Z_1 \dots Z_d)$ be d random variables with PDF $\rho(\mathbf{Z})$ that parameterize ice
  - Let $\{\Phi_k\}$ denote the set of polynomials which are orthogonal w.r.t. $\rho(\mathbf{Z})$
  - Let $y(\mathbf{Z})$ denote the mapping from $\mathbf{Z}$ to an aerodynamic performance metric
- **Probabilistic Collocation Method:**
  - *Representation*

$$y(\mathbf{Z}) \approx \sum_{|i|=0}^{N} y_i \Phi_i(\mathbf{Z})$$

  - *Orthonormality*

$$\langle f, g \rangle = \int_{\Gamma} f(\mathbf{z}) g(\mathbf{z}) \rho(\mathbf{z}) d\mathbf{z}$$

$$\langle \Phi_i, \Phi_j \rangle = \delta_{ij}$$

  - *Quadrature*

$$y_k = \langle y, \Phi_k \rangle \approx \sum_{i=0}^{Q} y(\mathbf{Z}^{(k)}) \Phi_k(\mathbf{Z}^{(k)}) w_k$$

[4] Xiu D. *Numerical Methods for Stochastic Computations: A Spectral Method Approach*. Princeton University Press, 2010.

PCE with Sparse Grids

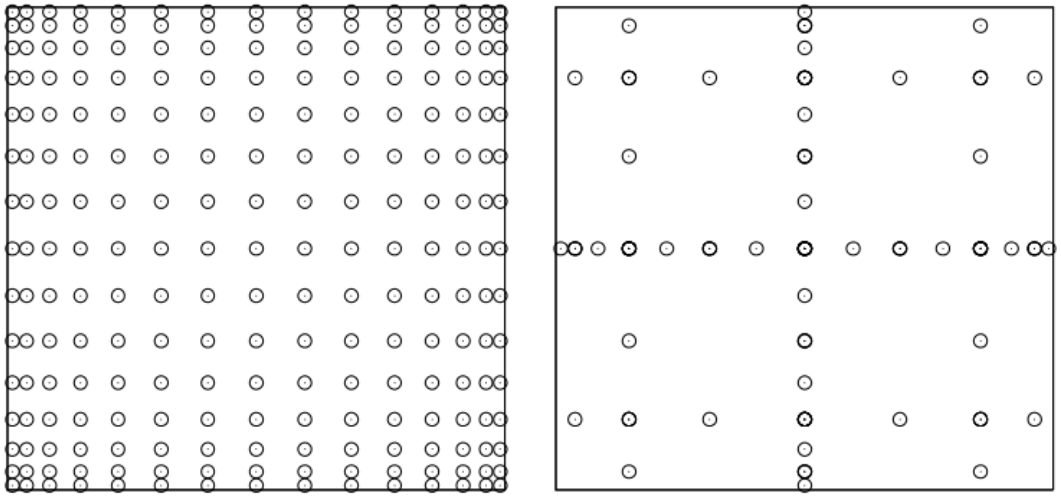

Full Tensor Product vs. Sparse Grid

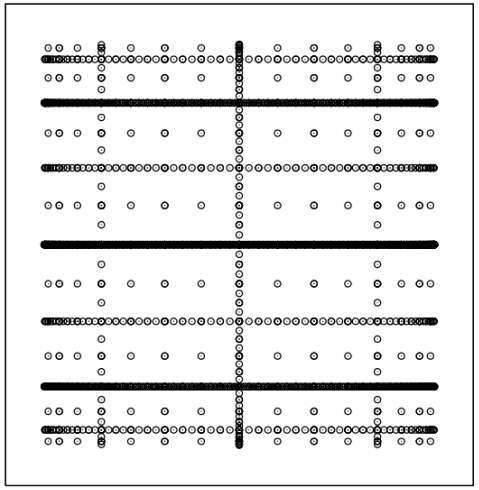

Anisotropic Grid

- **Sparse Grids**[5]
  - *Efficient*: Only a subset of the full quadrature grid is used
    - For $d >> 1$, number of samples scales as $2^N \binom{N+d}{d} << (N+1)^d$
  - *Adaptive*: Start with a coarse mesh, adaptively refine until achieve desired resolution
  - *Anisotropic*: Refine grid in most "important" directions
  - Implemented in DAKOTA[6] (open-source UQ code)

[5] LeMaitre O. *Spectral Methods for Uncertainty Quantification*. Springer, 2010.

[6] Adams et. al. *DAKOTA, A Multilevel Parallel Object-Oriented Framework for Design*

Topic

1. Icing: Introduction/Methodology
2. Icing: UQ Examples
3. Icing: Computational-Based UQ
4. Fires: Introduction/Methodology
5. Fires: Example study

Heuristic Input Processes

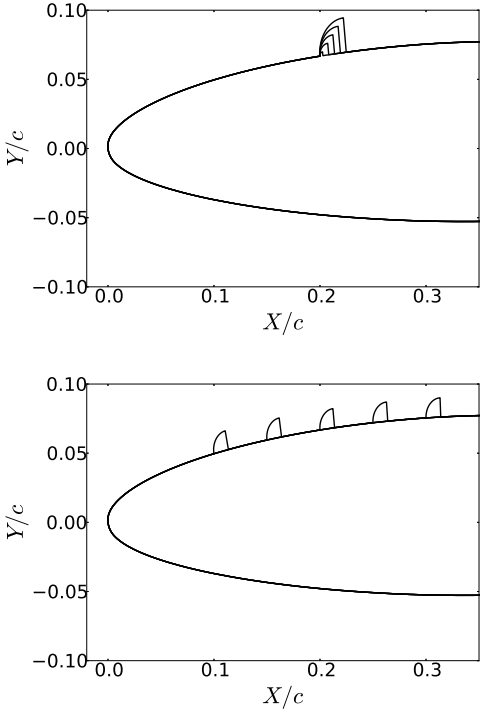

Ridge

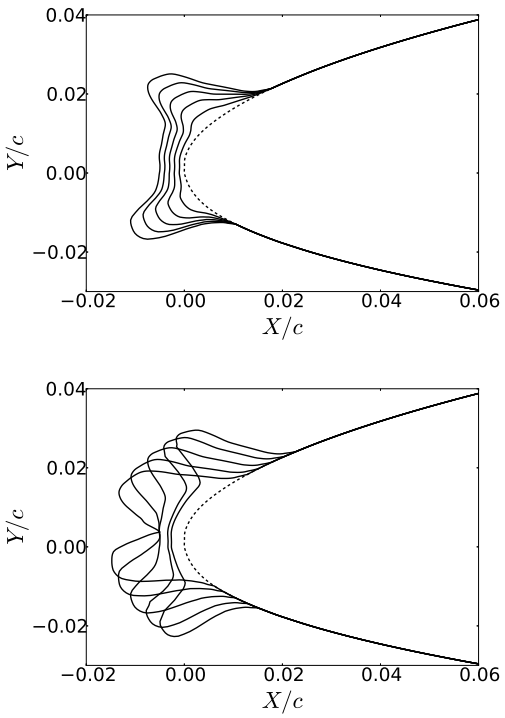

Horn

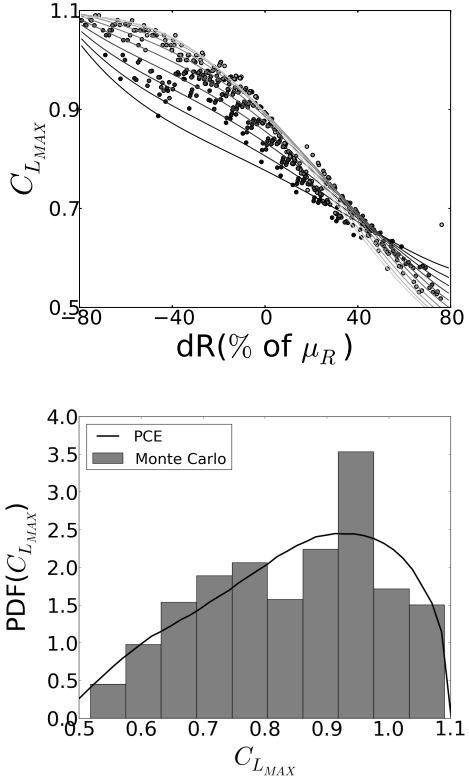

Statistics

- Heuristic approach[7]
- 2-D shape parameter space

[7] DeGennaro A., Rowley C.W., and Martinelli, L. *Uncertainty Quantification for Airfoil Icing using Polynomial Chaos Expansions*. To appear in Journal of Aircraft, 2015.

Data-Based Input Processes: 3D Wing

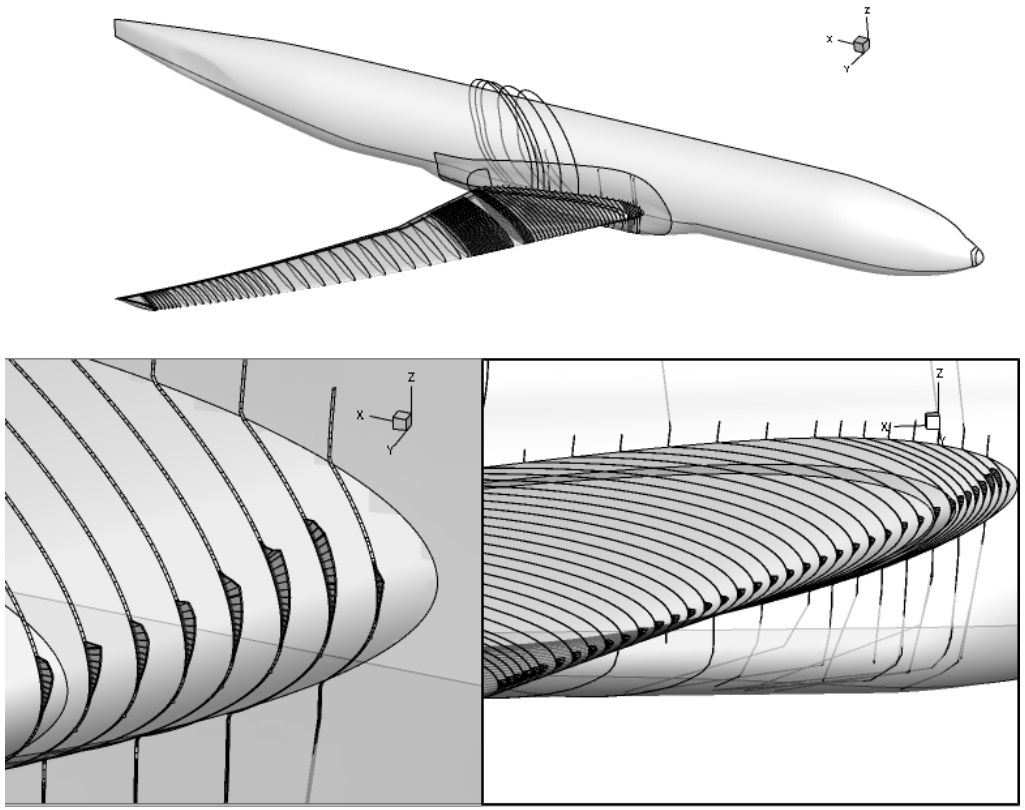

- NASA Common Research Model (CRM), 65% scale[8]
  - 45 min accretion time, altitude = 10,000 ft, velocity = 232 knots, temperature = -4° C, MVD = 20 μm, LWC = 0.55 g/m^3

[8] Broeren A. et. al. *Swept-Wing Ice Accretion Characterization and Aerodynamics*, AIAA 2013-2824.

Data-Based Input Processes: 3D Wing

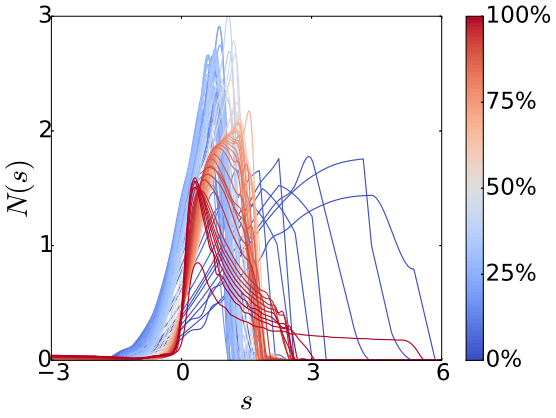

Original Data

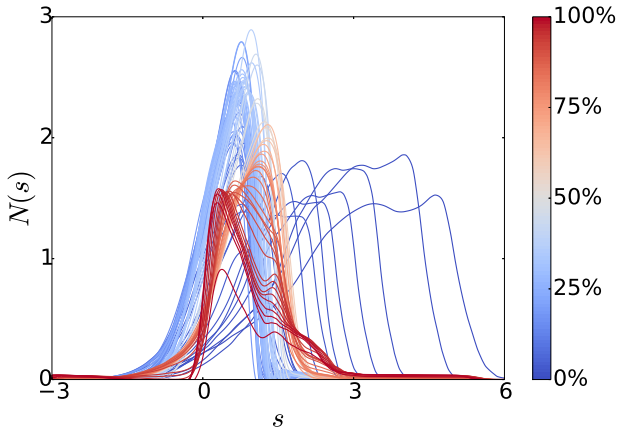

POD Reconstruction

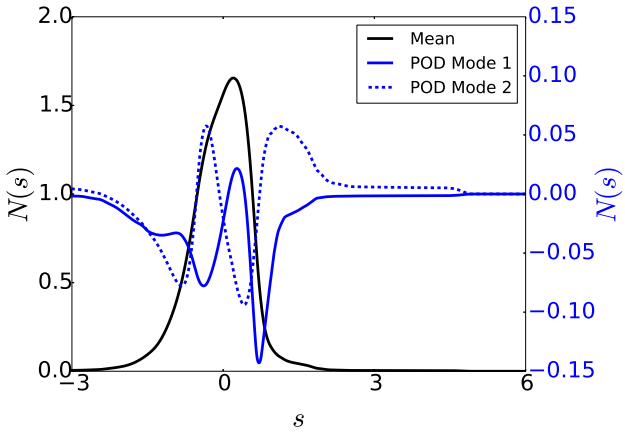

POD Modes

$$N(s) = h\{\bar{N}(as+b) + \sum_{i=1}^{2} c_i \Phi_i(as+b)\}$$

- h, a, b are scaling parameters
- c_1, c_2 are POD coefficients
- This collapses 100 different snapshots into 5 parameters

Data-Based Input Processes: 3D Wing

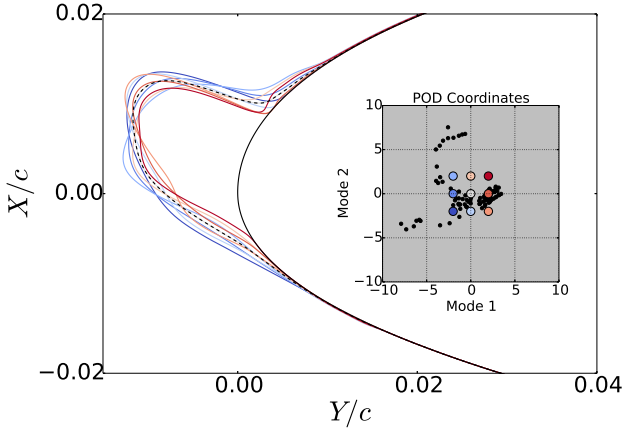

POD Modes

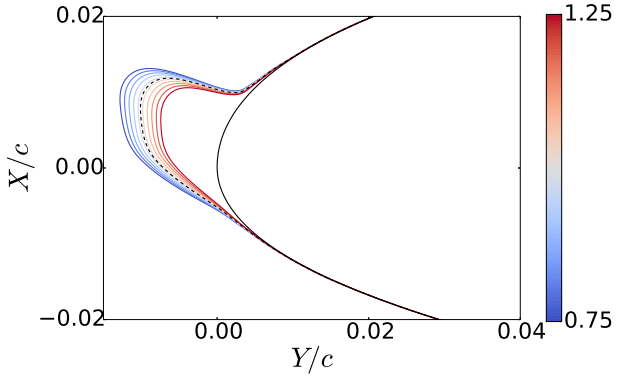

Height

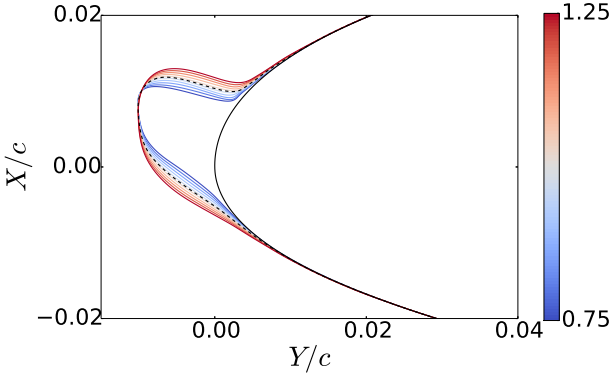

Width

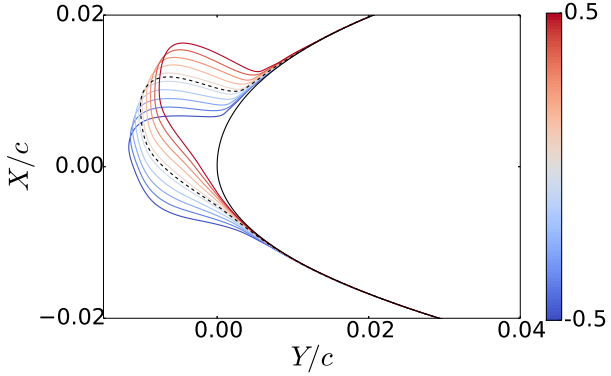

Position

- 2 POD coefficients (*shape*) + width, height, position parameters (*scaling*)

Data-Based Input Processes: 2D Shapes

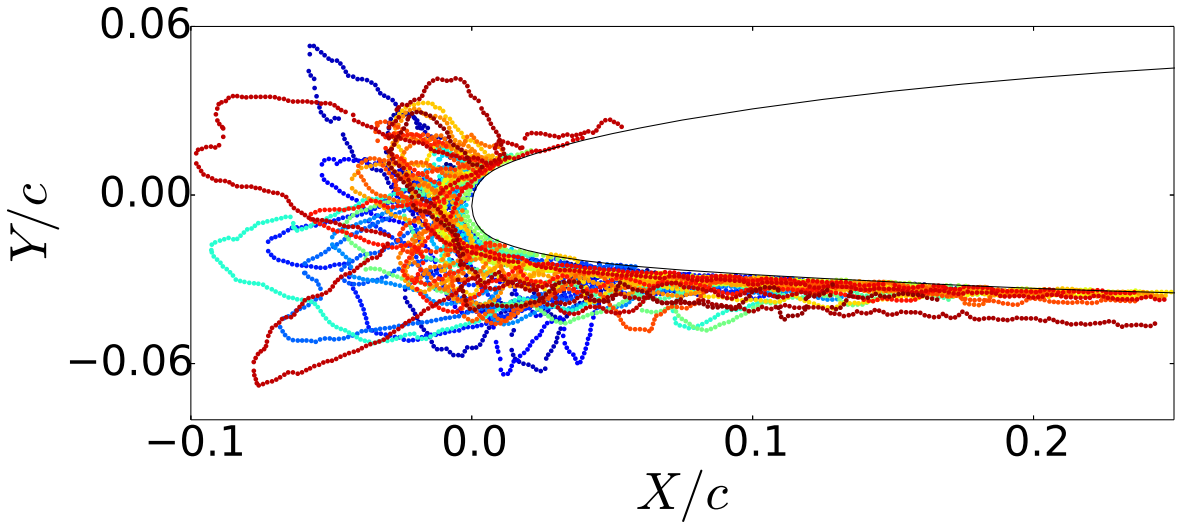

- Business jet clean airfoil geometry[9]
- 54 ice shapes, exposed to wide range of various icing conditions consistent with FAA certification guidelines
- POD dataset will consist of binary values defined on a static Cartesian mesh ('1' if mesh point is on the ice, '0' if not)

[9] Addy, H.E. *Ice Accretions and Icing Effects for Modern Airfoils*. NASA TR 2000-210031.

Data-Based Input Processes: 2D Shapes

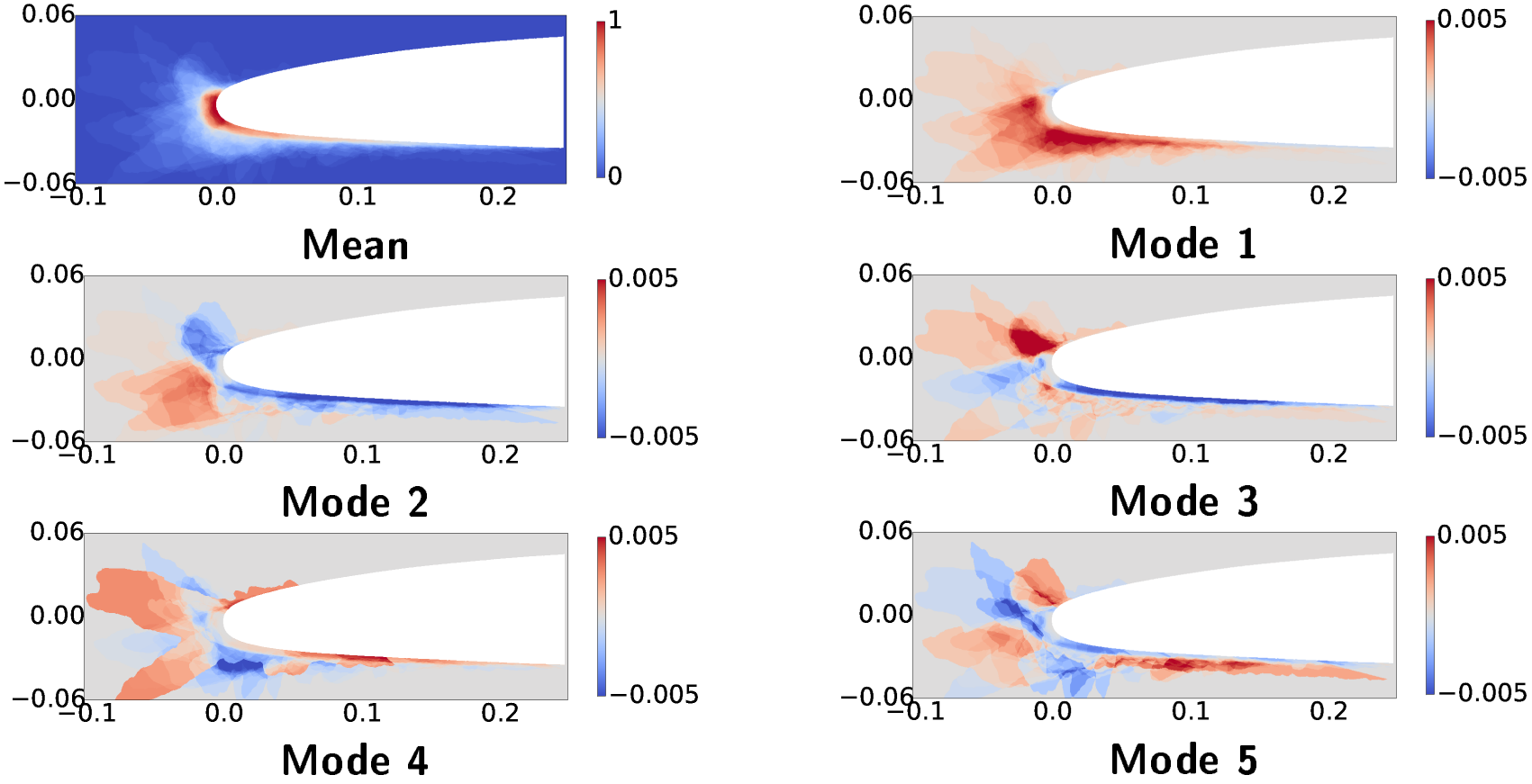

- 8 Modes retained; this is where POD eigenvalue magnitudes have decayed by an order of magnitude

Data-Based Input Processes: 2D Shapes

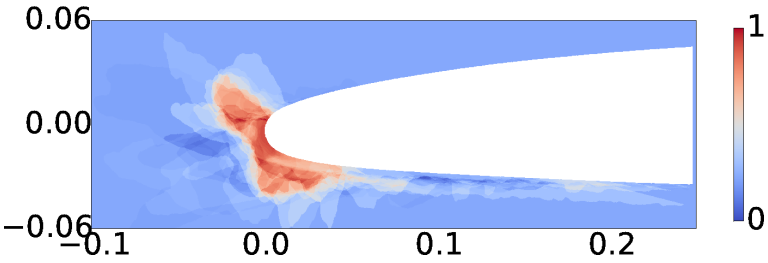

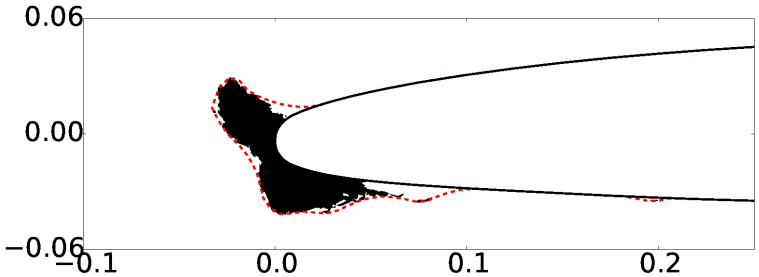

Unfiltered Reconstruction

Filtered Reconstruction

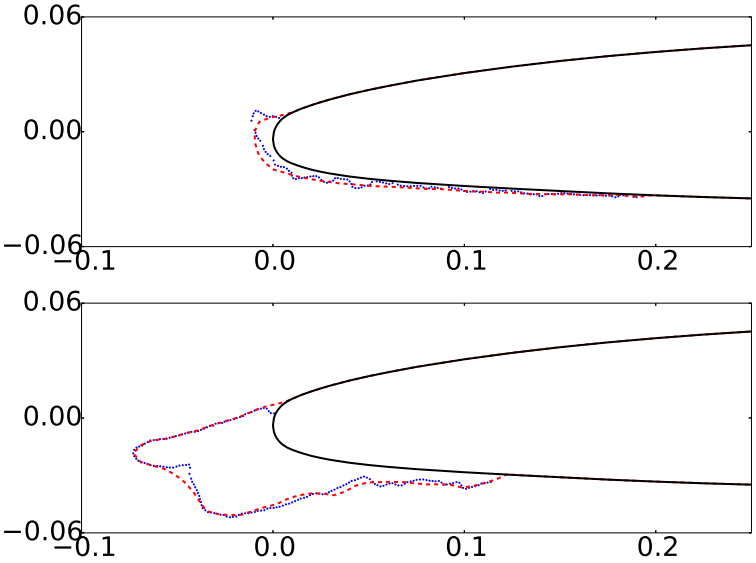

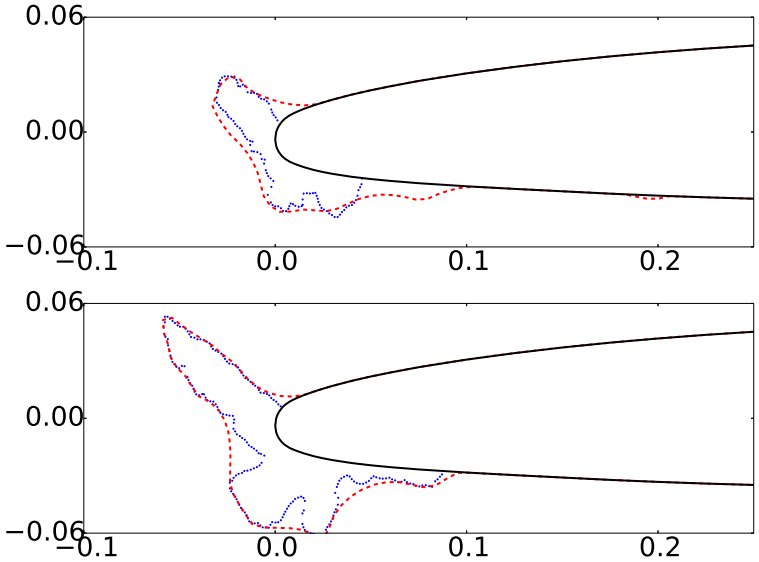

Ice Reconstructions

Statistics: 3D Wing

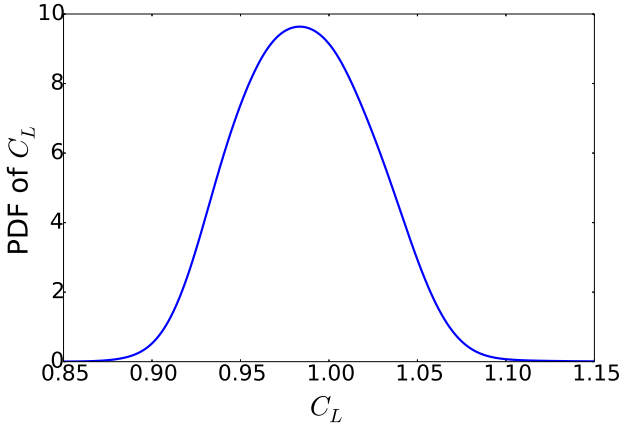

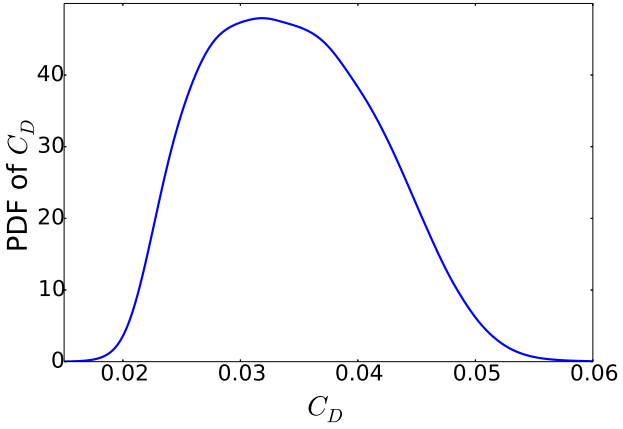

C_L Statistics **C_D Statistics**

	Width	Position	Height	POD 1	POD 2
T (C_L)	0.03	0.69	0.15	0.11	0.14

- Our surrogate is an explicit polynomial function of the input variables, making statistical inference easy/quick
- PCE surrogate computed using 1,103 sparse grid points
- Sobol index $T_i = \frac{\mathbb{E}[Var(Y|Z_{-i})]}{Var(Y)}$ is a measure of how much Z_i contributes to the total variance of $Y(\mathbf{Z})$
- For our parameter ranges, position perturbation accounts for most of the statistical variation

Statistics: 3D Wing

- Analyze statistical clustering of horns that produce bottom and top 10% of C_L variation

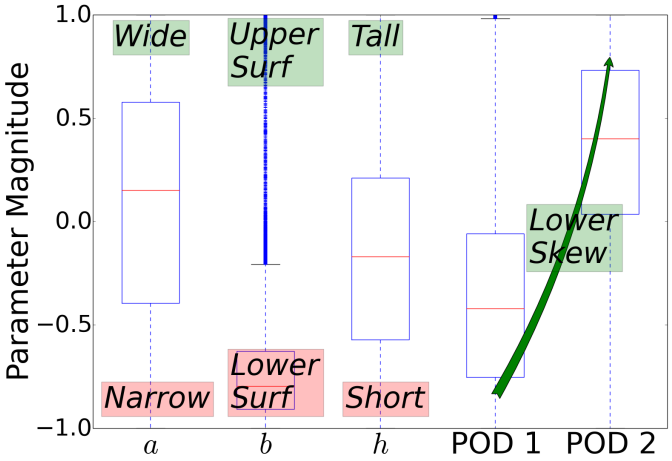

Favorable Horns

- Wider/rounded
- Lower surface
- Shorter
- Gentle downward skew

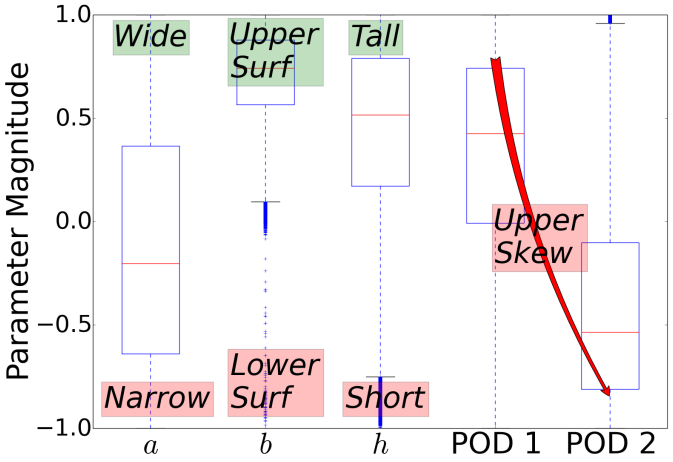

Unfavorable Horns

- Sharper/narrower
- Upper surface
- Taller
- Sharp, upper skew shape

Flow Solutions

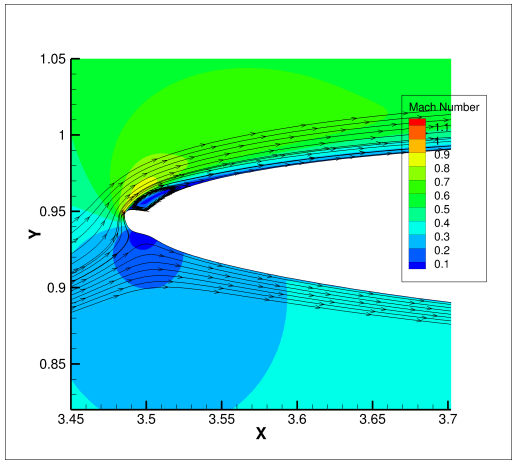

Favorable Position

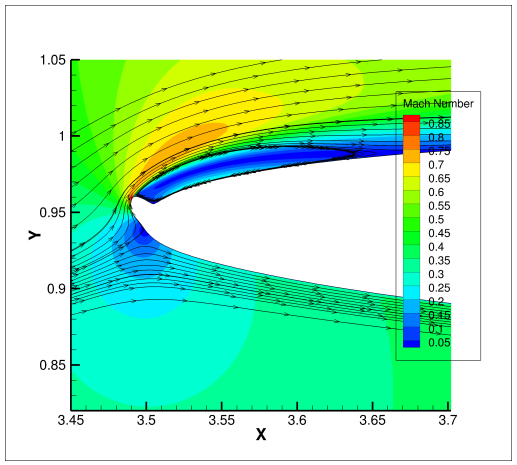

Unfavorable Position

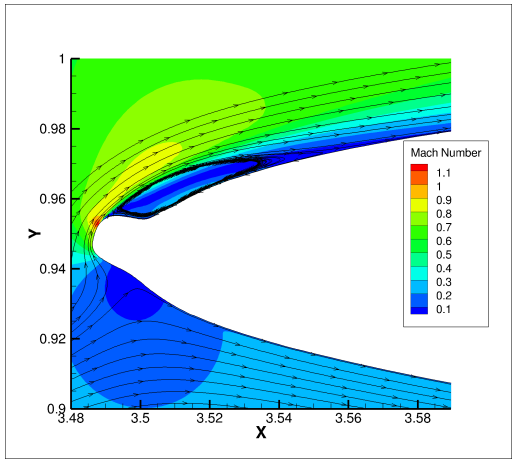

Favorable shape skew

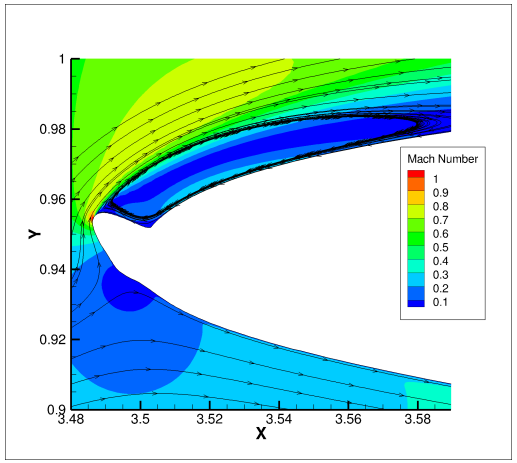

Unfavorable shape skew

Topic

1. Icing: Introduction/Methodology
2. Icing: UQ Examples
3. Icing: Computational-Based UQ
4. Fires: Introduction/Methodology
5. Fires: Example study

Motivation

- **Investigate uncertainty in the physical process of icing**
  - What is the statistical effect of uncertainty in physical parameters?
    - Free-stream temperature
    - Angle of attack
    - Convective heat transfer
    - Droplet diameter distribution
    - Accretion time

Airfoil Icing Code Flowchart

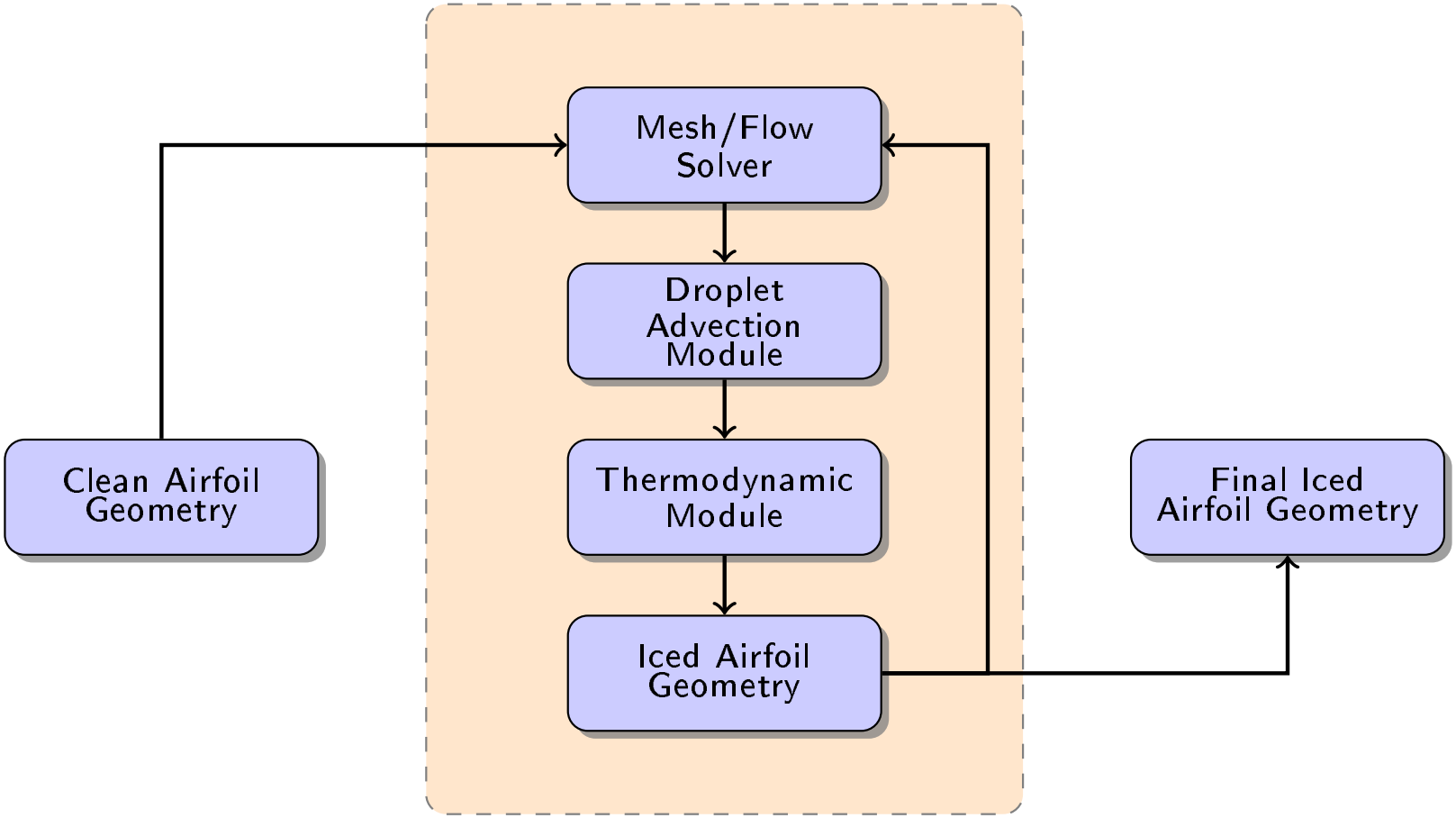

Droplet Advection

$$\frac{d\mathbf{x}}{dt} = \mathbf{v}$$

$$m\frac{d\mathbf{v}}{dt} = \frac{1}{2}\rho_g C_D \pi r^2 ||\mathbf{v_g} - \mathbf{v}||(\mathbf{v_g} - \mathbf{v}) + m\mathbf{g}$$

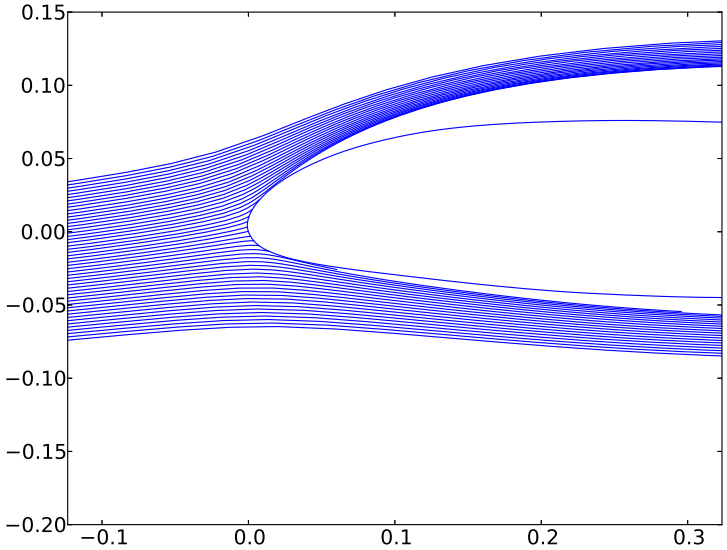

$\mathbf{R = 10\mu m}$

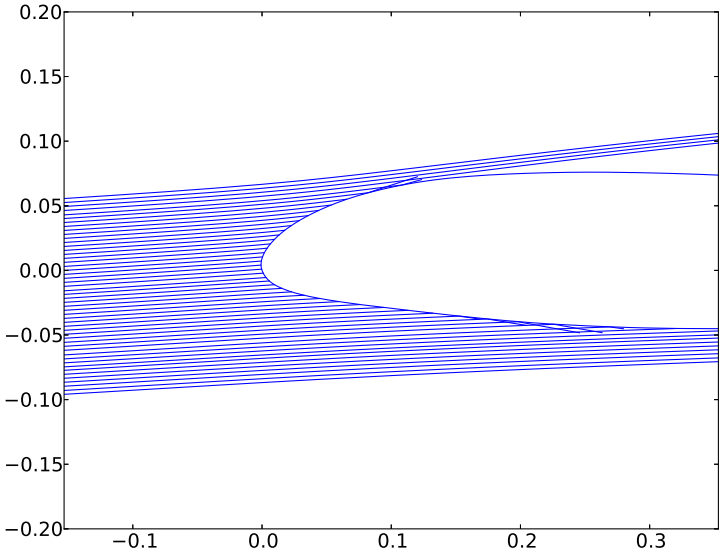

$\mathbf{R = 100\mu m}$

Thermodynamics

$$\rho_w \left\{ \frac{\partial h_f}{\partial t} + \nabla \cdot (\mathbf{u_f} h_f) \right\} = \dot{m}_{imp} - \dot{m}_{ice}$$

$$\rho_w \left\{ \frac{\partial (h_f c_W T)}{\partial t} + \nabla \cdot (\mathbf{u_f} h_f c_W T) \right\} = \left[c_W T_d + \frac{u_d^2}{2} \right] \dot{m}_{imp} + (L_{fus} - c_{ice} T) \dot{m}_{ice} + c_H (T_\infty - T)$$

- **Mass**
  - Enters through impinging droplets
  - Exits via evaporation/sublimation and freezing
- **Energy**
  - Enters through impinging droplets, freezing of ice
  - Exits via evaporation/sublimation, radiation, convection
- Solved explicitly using finite volume discretization with Roe scheme upwinding

Preliminary Intermediate Results: Ice Shapes

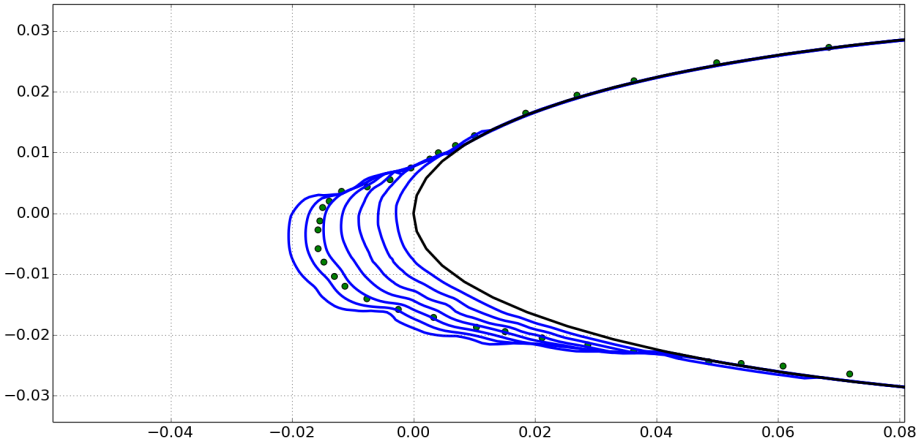

- NACA0012, $\alpha = 4^o$, $T_\infty = 256K$, $U_\infty = 103$ m/s, MVD = 20 μm, LWC = 0.55 g/m^3, Re = 4.14 million, $\Delta T = 7$ min
- Low temperatures: convective heat transfer high enough to freeze all incoming droplets instantly (rime)

Work In-Progress

- Implement rough-wall extension in Spalart-Almaras turbulence model
- Implement neglected mass/energy transfer mechanisms
- Verify icing calculations against published results
- Perform UQ studies, investigate sensitivity to physical parameters
  - Temperature, convective heat transfer coefficient, Reynolds number, MVD, LWC, angle of attack, etc.

Topic

1. Icing: Introduction/Methodology
2. Icing: UQ Examples
3. Icing: Computational-Based UQ
4. Fires: Introduction/Methodology
5. Fires: Example study

Motivation

- **Cargo hold fires are a significant safety hazard**
  - Tight constraints for detection/suppression
  - FAA requires detection of cargo fire within 60 seconds of ignition[10, 11]

Cargo hold fire generated from lithium-ion battery

Cargo hold fire generated from e-tablet

[10] Blake, D. et. al. 2014 Fire Safety Highlights. Federal Aviation Administration. Research Summary, 2014.

[11] Oztekin, E. S. Heat and mass transfer due to a small-fire in an aircraft cargo compartment. Journal of Heat and Mass Transfer Vol. 73, 2014, pp. 562-573.

Motivation

- **Current detection systems are overly conservative**[12]
  - 200-to-1 false alarm ratio (1995-99)
  - Unscheduled landings are expensive

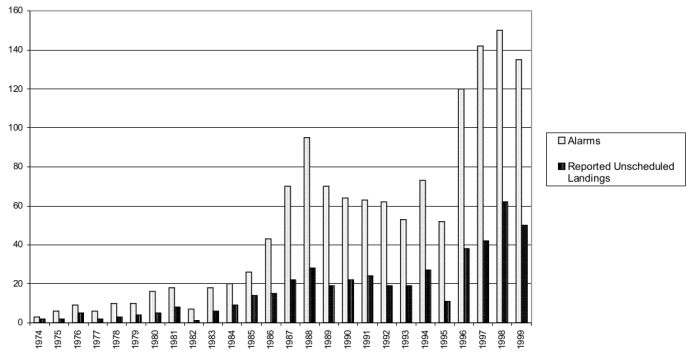

Alarms and Unscheduled Landings

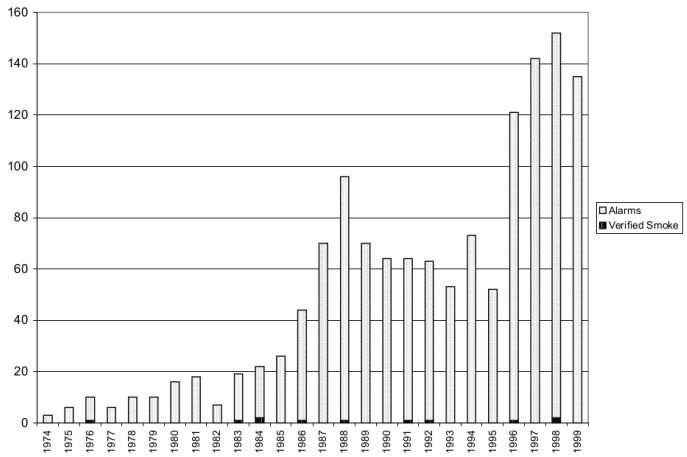

False/Verified Alarms

[12] Blake. Aircraft cargo compartment smoke detector alarm incidents on U.S.-registered aircraft. *FAA technical note* FAA-TN00/29, 2000.

Motivation

- **Fire dynamics are sensitive to boundary condition uncertainty**
  - Fire source location and temperature within cargo hold can vary
  - Cargo hold is cluttered with baggage, packages, pipes, etc.
  - Spatio-temporal fire plume development is affected by this uncertainty

Cargo hold clutter

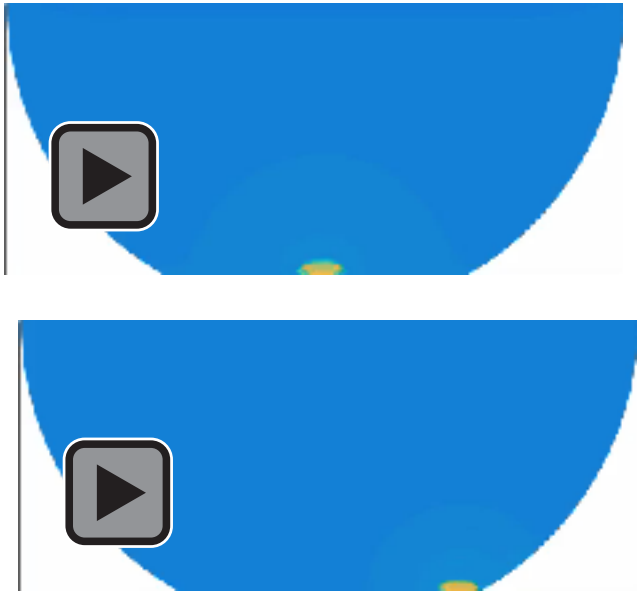

Effect of Source Position

Motivation

- **Experiments are expensive**
  - Destructive full-scale cargo hold fire experiments (FAA Tech Center)[13]
  - Each experiment destroys an entire cargo hold
  - Investigating boundary condition uncertainty is not feasible

Boeing 707 cargo hold

Destructive cargo hold fire experiment

[13] Oztekin, E. S. Modeling of smoke spread and gas transport in an aircraft. 7th International Fire and Cabin Safety Research Conference, 2013.

Motivation

- **Computational methods must be accurate**
  - Previous attempts at applying CFD to cargo hold fires have used low-order finite-volume solvers on meshes that do not conform to boundary[14]

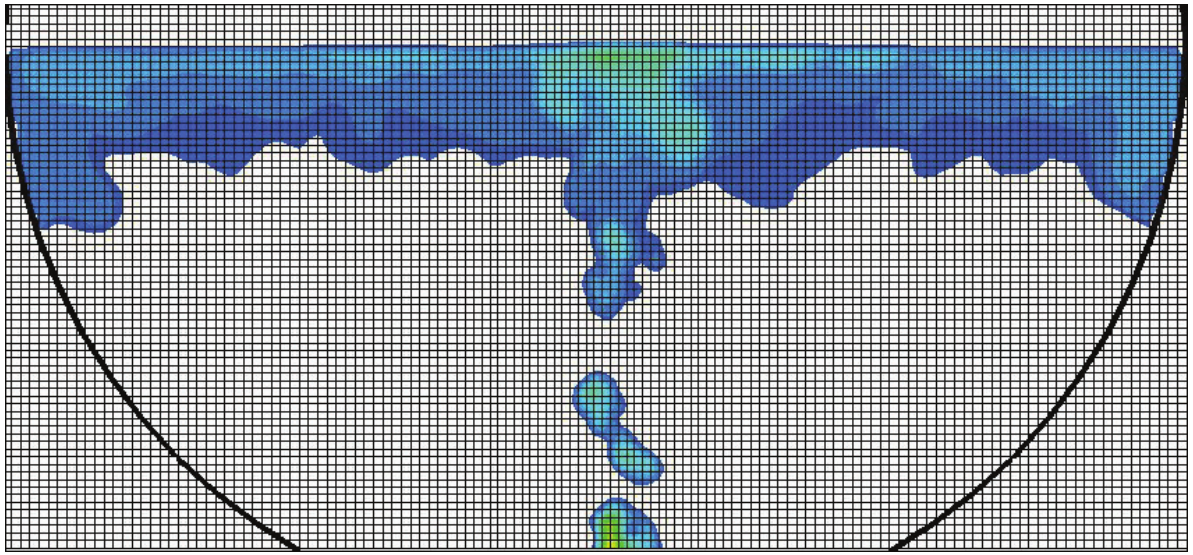

Non-conformal Cartesian mesh

[14] Oztekin, E.S et. al. Flow induced by a small fire in an aircraft cargo compartment. AIAA 2012-0311.

Motivation

- **Computational methods must be accurate**
  - Vorticity dominated, buoyancy-driven flows require high computational accuracy

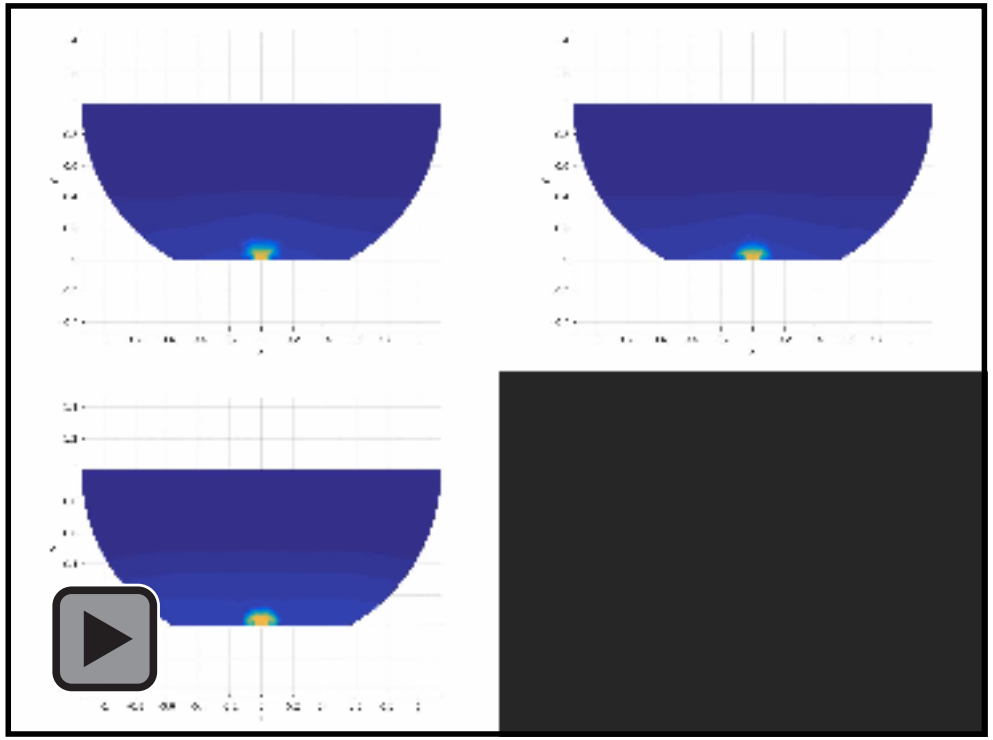

Discontinuous Galerkin using varying degrees of accuracy

Objectives

- **Apply accurate CFD tools to the cargo hold problem**
  - Boundary-fitted meshes for good boundary resolution
  - Discontinuous Galerkin (DG) high-order method for high accuracy
- **Apply UQ tools to study effects of uncertainty in cargo hold problem**
  - Polynomial Chaos Expansions (PCE)
  - Efficient sampling methodology
  - Accurate surrogate construction
- Methodology gives (1) accurate computational tool for simulating cargo hold fires and (2) efficient framework for investigating cargo hold uncertainty

Discontinuous Galerkin (DG) Method

- High-resolution CFD method[15, 16]
  - Domain is divided into cells, collocation nodes computed within each cell
  - N-S equations projected onto span of polynomials (of arbitrary degree)
  - Flow variables within each cell represented in polynomial basis

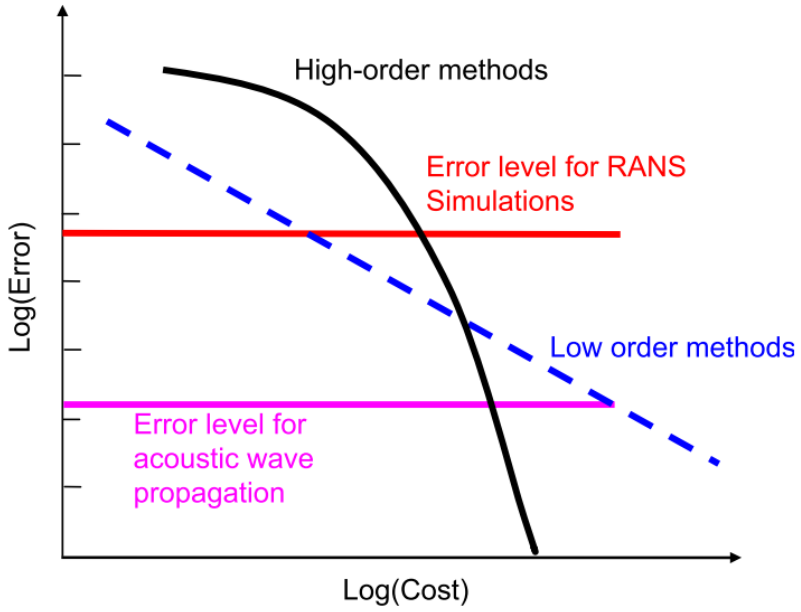

Generic error vs cost plot

[15] Wang et. al. An eulerian-lagrangian DG method for transient advection-diffusion equations. *Numerical Methods for Partial Differential Equations*, 2007.

[16] Hesthaven & Warburton. *Nodal Discontinuous Galerkin Methods*, 2008.

Discontinuous Galerkin (DG) Method

Method Synopsis

Conservation law: $$\frac{\partial \mathbf{u}}{\partial t} + \nabla \cdot \mathbf{f}(\mathbf{u}) = 0$$

Weak formulation: $$\int_V \frac{\partial \mathbf{u}}{\partial t}\phi_j \; dV + \int_V \nabla \cdot \mathbf{f}(\mathbf{u})\phi_j \; dV = 0$$

Integrate by parts: $$\int_V \frac{\partial \mathbf{u}}{\partial t}\phi_j \; dV - \int_V \nabla\phi_j \cdot \mathbf{f} \; dV + \oint_S \phi_j \hat{\mathbf{f}} \cdot \hat{\mathbf{n}} \; dS = 0$$

$\mathbf{u} \approx \sum \mathbf{u}_i \phi_i$: $$\int_V \frac{\partial \mathbf{u}_i \phi_i}{\partial t}\phi_j \; dV - \int_V \nabla\phi_j \cdot \mathbf{f}_i \phi_i \; dV + \oint_S \phi_j \hat{\mathbf{f}}_i \phi_i \cdot \hat{\mathbf{n}} \; dS = 0$$

$$\mathbf{M}_{ij}\frac{d\mathbf{u}_i}{dt} = \int_V \nabla\phi_j \cdot \mathbf{f}_i \phi_i \; dV + \oint_S \phi_j \hat{\mathbf{f}}_i \phi_i \cdot \hat{\mathbf{n}} \; dS$$

Polynomial Basis

- Collocation nodes are defined in each individual cell
- Chebyschev-like schemes used (to avoid Runge-phenomenon)
- Associated Lagrange interpolators form the polynomial basis ϕ_k

Discontinuous Galerkin (DG) Method

Time-Stepping

- We now have a system of ODEs to solve for each DG mode:

$$\frac{d\mathbf{u}}{dt} = \mathbf{f}(\mathbf{u}, \mathbf{u}', \mathbf{t})$$

- CFL condition for explicit time-stepping gives $\Delta t = O(\frac{\Delta x}{N^2})$
  - Mesh volume Δx can be small
  - State dimension N grows rapidly with increasing polynomial order
- Thus, implicit time-stepping is used, which gives the large nonlinear system:

$$\mathbf{F}(\mathbf{u}) = 0$$

Discontinuous Galerkin (DG) Method

Solution Procedure

- Newton's method gives sequence of linear systems:

$$\mathbf{J}(\mathbf{u}^k)\delta\mathbf{u}^k = -\mathbf{F}(\mathbf{u}^k), \quad \mathbf{u}^{k+1} = \mathbf{u}^k + \delta\mathbf{u}^k$$

- $\mathbf{J}$ is prohibitively large to compute/store
- Jacobian-Free Newton-Krylov iteration
  - Action of Jacobian on a vector is approximated as:

$$\mathbf{J}\mathbf{v} \approx [\mathbf{F}(\mathbf{u} + \epsilon\mathbf{v}) - \mathbf{F}(\mathbf{v})]/\epsilon$$

  - $\delta\mathbf{u}^k$ is solved for using Krylov iteration (GMRES, BiCGSTAB)

Polynomial Chaos Expansions (PCE)

- Overview[17]:
  - Method for quantifying parametric uncertainty
  - Expand output in terms of basis polynomial functions of random variables

$$f(\xi) \approx \sum_{i}^{N} a_i \psi_i(\xi)$$

- Pros:
  - Efficient sampling methodology
  - Explicit surrogate model
  - Easy statistical post-processing (eg., sampling, ANOVA)

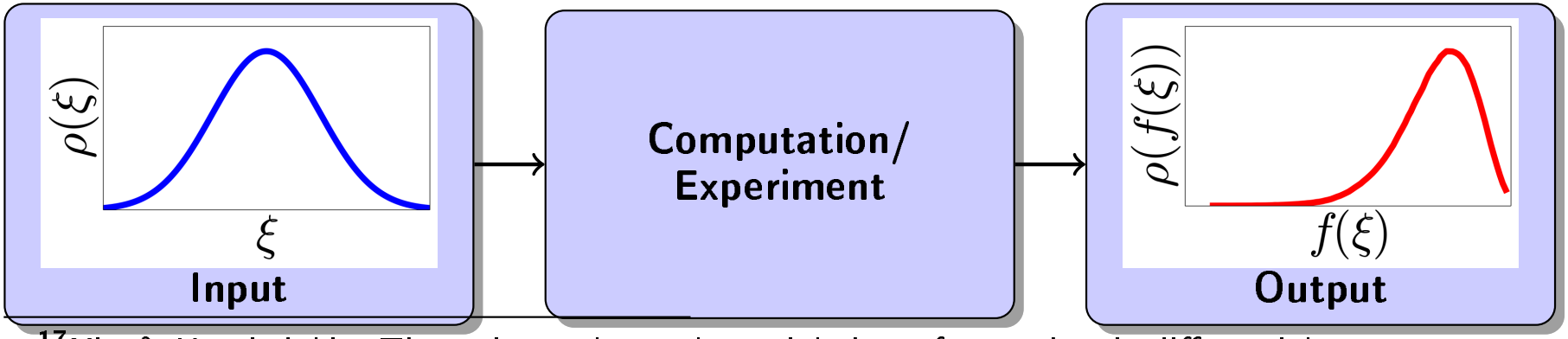

[17] Xiu & Karniadakis. The weiner-askey polynomial chaos for stochastic differential equations. *SIAM Journal of Scientific Computing*, 2002.

Polynomial Chaos Expansions (PCE)

Setting

- Stochastic input process parameterized by d independent random variables $\xi_1 \cdots \xi_d$ with joint PDF $\rho(\xi)$
- Objective: approximate statistical dependence of an output variable $f(\xi)$

Method Synopsis

Polynomial basis: $\{\psi_k\}_{k=1}^{\infty} \quad , \quad \langle \psi_i, \psi_j \rangle = \delta_{ij}$

$$\langle f, g \rangle = \int_{\Gamma} f(\xi) g(\xi) \rho(\xi) d\xi$$

Output Representation: $f(\xi) \approx \sum_{i}^{N} a_i \psi_i(\xi)$

Projection: $a_k = \dfrac{\langle f, \psi_k \rangle}{\|\psi_k\|^2}$

Quadrature: $\langle f, \psi_k \rangle \approx \sum_{i=1}^{Q} f(\xi^i) \psi_k(\xi^i) w^i$

Polynomial Chaos Expansions (PCE)

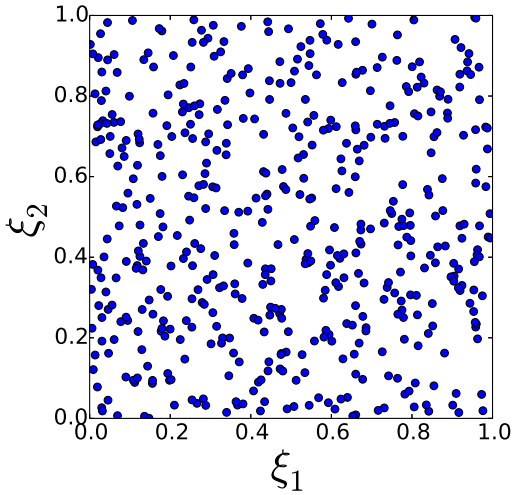

Monte Carlo

$$y \approx \delta(\xi - \xi_k)$$

- Draw random samples
- Data exist at discrete points

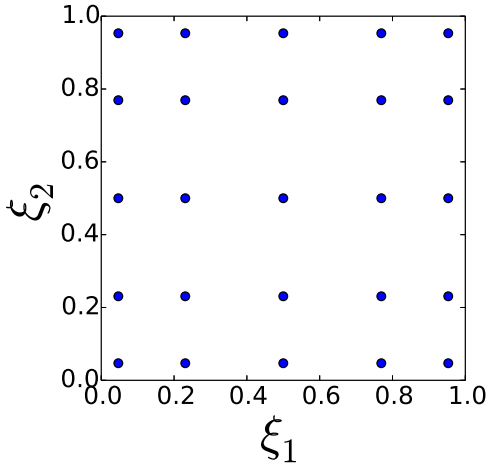

Polynomial Chaos

$$y \approx \sum_{i}^{Q} c_i \psi_i(\xi)$$

- Take data at collocation points
- Construct global surrogate

Topic

1. Icing: Introduction/Methodology
2. Icing: UQ Examples
3. Icing: Computational-Based UQ
4. Fires: Introduction/Methodology
5. Fires: Example study

Input Processes

Parameters: Fire source temperature and location

- Empty cargo hold
- Uniform distribution for both independent parameters

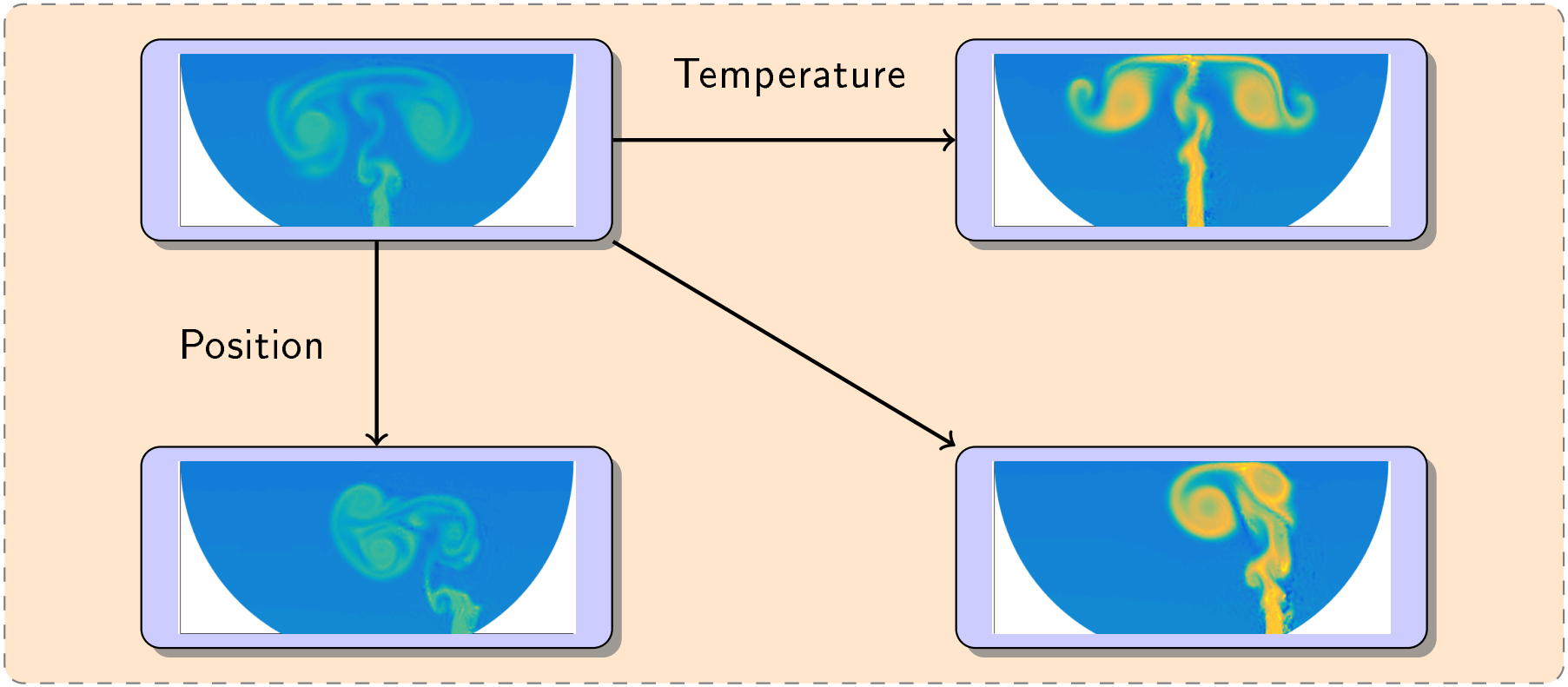

Input Processes

Parameters: Fire source temperature and location

- Empty cargo hold
- Uniform distribution for both independent parameters

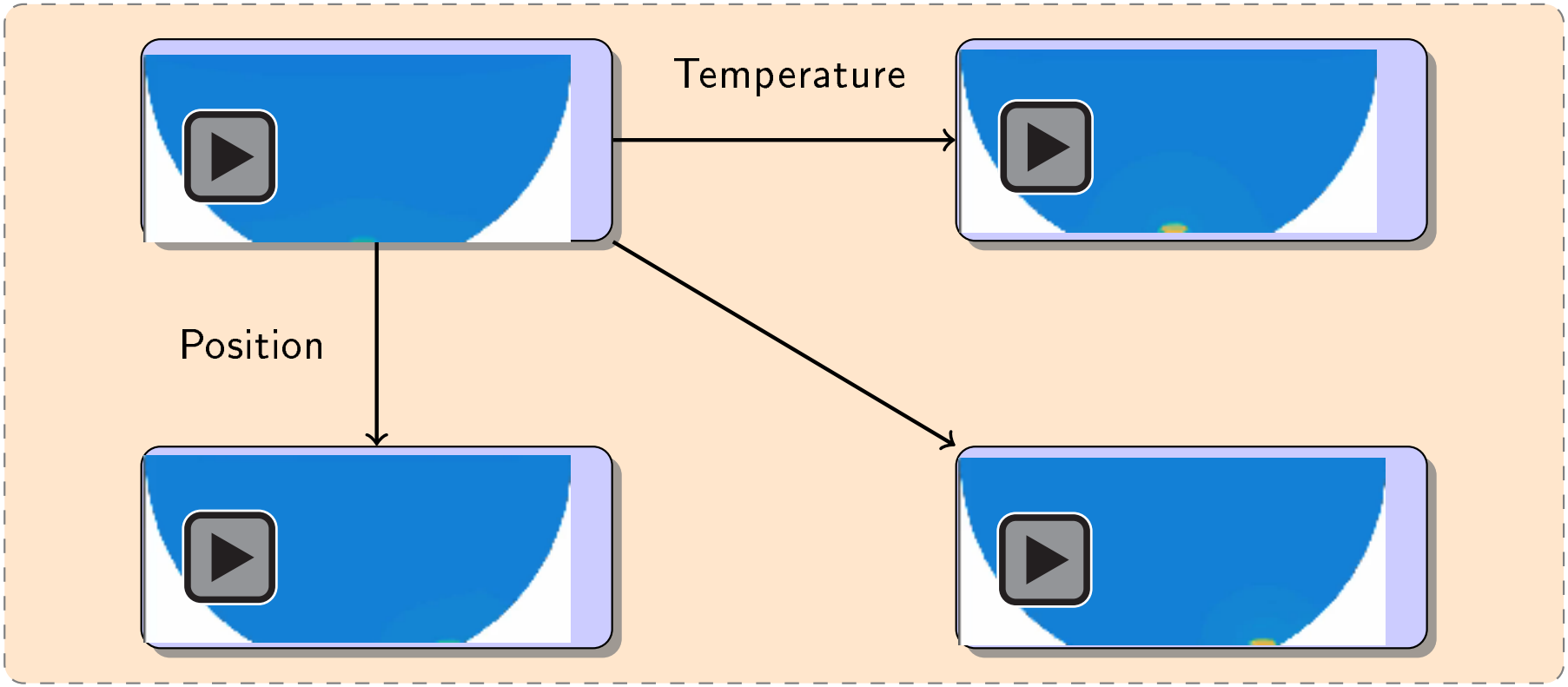

Output Measurements

Problem

- UQ for the entire flow field is difficult
  - Spatio-temporal behavior varies significantly
  - Need a more tractable set of observables

Solution

- Reduce spatial dimensionality
  - Ceiling temperature is most important for detection
- Separate time and space
  - *Intuition*: buoyant plumes convect upwards at some characteristic time t_R dominated by source temperature
  - Easier to compare ceiling temperatures at their respective values of t_R than at same time after ignition

Output Measurements

$$t_R(Z) = (\text{Rise time})$$

$$T_C(x; Z) = \frac{1}{\Delta t} \int_{t_R(Z)}^{t_R(Z)+\Delta t} T_C(x, t; Z)\, dt$$

Results: Rise Time

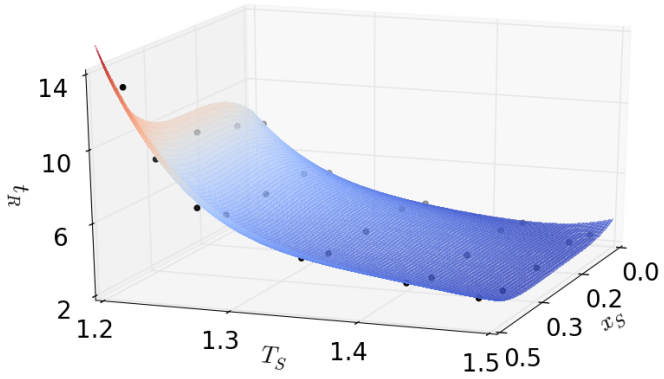

PCE surrogate map of $t_R(Z)$

- t_R is dominated by source temperature
- Clearly, hotter source gives shorter rise time

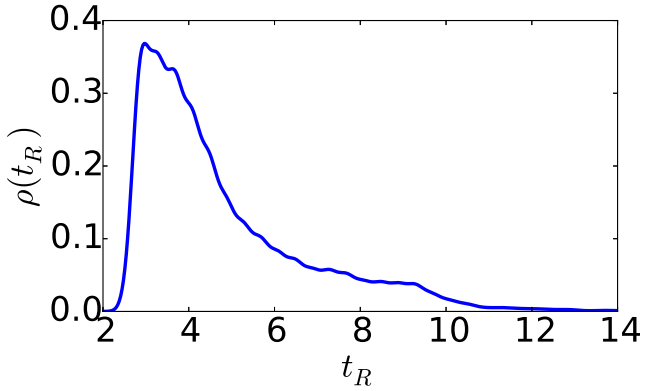

Probability density function

- Nonlinear mapping deforms (initially uniform) PDF
- Tail caused by low temperature and wall effect

Results: Ceiling Temperature

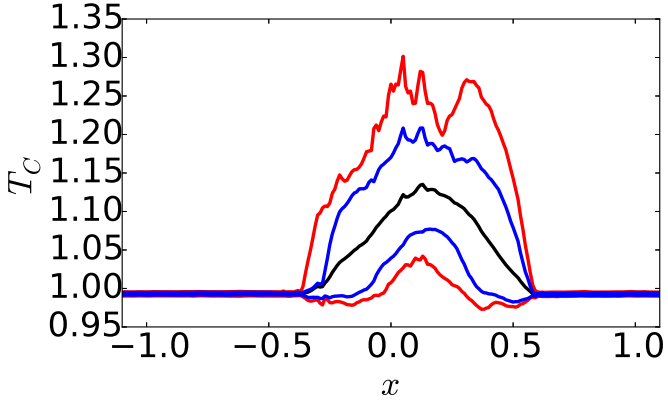

Mean and Confidence Intervals

- (68%, 95%) C.I.
- Profile skewed right of center
- Wide variation in temperature range and locations possible

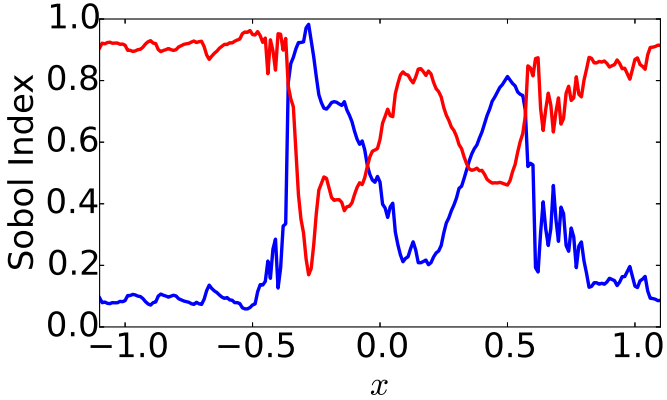

Sobol indices

- (x_S, T_S)
- Fraction of variance attributable to each individual parameter
- T_S: dominant near maximum
- x_S: dominant near periphery

Results: Related Statistics

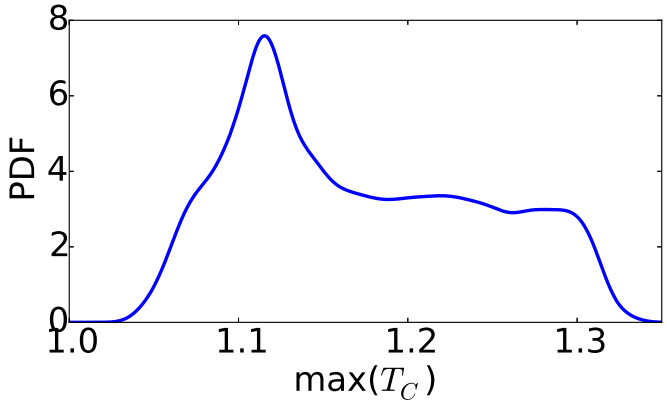

PDF of max(T_C)

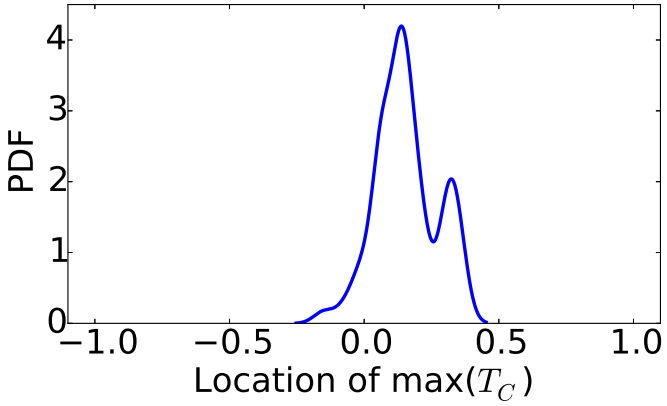

PDF of Location(max(T_C))

- Can estimate statistics of quantities derived from output measurements
- The maximum ceiling temperature and its location are of practical engineering interest
- For this example, a temperature sensor must:
  - Be able to detect temperatures roughly in the range $T_C \in [1.05, 1.35] \times T_\infty$
  - Be placed on the ceiling in roughly in the range $x_C \in [-0.25, 0.5]$

Conclusions/Future Work

Problem

- Airfoil icing/cargo hold fire safety is important and subject to uncertainty
- Experiments are expensive
- CFD methods must be high-resolution

Solutions: Icing

- Data-based modeling of shape variation
- Computational-based UQ

Solutions: Fires

- Discontinuous-Galerkin solver for high CFD resolution
- Polynomial Chaos for efficient sampling and accurate surrogate/statistics

Future Work: Fires

- Cargo holds in practice are not empty
- Extend framework to handle cargo hold clutter (baggage, pipes, etc.)

Future Work: Icing

- Extend efforts to 3D wing icing
- Continue development and testing of icing code
- Use icing code to investigate statistical variation of ice shape